



A Comparative Performance Analysis of Wireless Power Transfer with Parametric Simulation Approach

Mehmet Cicek^a, Selami Balci^{b*}, Kadir Sabanci^b

^a Department of Electrical and Electronics Engineering, Institute of Science, Gazi University, Ankara, Türkiye

^b Department of Electrical and Electronics Engineering, Faculty of Engineering, Karamanoglu Mehmetbey University, Karaman, Türkiye

*Corresponding Author: sbalci@kmu.edu.tr

Received: May 17, 2023 ◆ Accepted: June 19, 2023 ◆ Published Online: June 21, 2023

Abstract: This paper presents using a parametric technique optimise and normalise approach for coreless Resonant Inductive Coupling Wireless Power Transfer (RIC-WPT) systems. The system under consideration is based on a compensated series-series (SS) circuit employing flat spiral coils. Moreover, the proposed approach aims to determine the optimal values for capacitors to achieve maximum efficiency during the operation of the RIC-WPT system. Three-dimensional (3D) flat spiral coils are modelled and subjected to parametric analysis with varying air-gaps using ANSYS-Electronics-Maxwell software with the Finite Element Method (FEM). Subsequently, a power electronics circuit employing a full-bridge inverter is designed using ANSYS-Simplorer software. The coils and the power electronics circuit are co-simulated with different parameter values. Consequently, based on the findings of the parametric simulation studies, the most efficient configuration for a Wireless Power Transfer (WPT) system is proposed, incorporating the design and standardization of power electronics components suitable for the specified operating frequency. The simulation results indicate that power transmission with an efficiency of approximately 74.31% is achieved when the air gap between the coils is set to 200 mm. Moreover, the co-simulation studies, involving different parametric values in power electronics circuit parameters and electromagnetic modelling parameters, provide valuable insights for WPT designs.

Keywords: Co-simulation, FEM, parametric simulation, wireless power transfer.

Öz: Bu makale, nüvesiz Rezonant Endüktif Kuplaj Kablosuz Güç Aktarımı (RIC-WPT) sistemlerini optimize etmek ve standart hale getirmek için parametrik tekniklerin kullanımını sunmaktadır. Ele alınan sistem, düz spiral bobinler kullanan kompanse edilmiş bir seri-seri (SS) devreye dayanmaktadır. Ayrıca, önerilen yaklaşım, RIC-WPT sisteminde maksimum verim elde etmek için kapasitörler için en uygun değerleri belirlemeyi amaçlamaktadır. Üç boyutlu (3D) yassı spiral bobinler, Sonlu Elemanlar Metodu (SEM) ile ANSYS-Electronics-Maxwell yazılımı kullanılarak modellenmiş ve farklı hava aralıklarıyla parametrik analize tabi tutulmuştur. Daha sonra, ANSYS-Simplorer yazılımı kullanılarak tam köprü evirici kullanan bir güç elektroniği devresi tasarlanmıştır. Bobinler ve güç elektroniği devreleri, farklı parametre değerleri ile simüle edilmiştir. Sonuç olarak, parametrik simülasyon çalışmalarının bulgularına dayanarak, belirtilen çalışma frekansına uygun güç elektroniği bileşenlerinin tasarımını ve standardizasyonunu içeren bir Kablosuz Güç Aktarımı (WPT) sistemi için en verimli konfigürasyon önerilmiştir. Simülasyon sonuçları, bobinler arası boşluk 200 mm olarak ayarlandığında yaklaşık %74,31 verimle güç iletiminin elde edildiğini göstermektedir. Ayrıca, güç elektroniği devre parametrelerinde ve elektromanyetik modelleme parametrelerinde farklı parametrik değerleri içeren eşanlı benzetim çalışmaları, WPT tasarımları için değerli bilgiler sunmaktadır.

Anahtar Kelimeler: Eş-benzetim, SEM, parametrik benzetim, kablosuz güç aktarımı.

1. Introduction

Wireless power transfer (WPT) systems have gained considerable attention in various domains, ranging from everyday devices such as toothbrushes to advanced applications like spacecraft. Resonant inductive coupling wireless power transfer (RIC-WPT) [1] represents a wireless power transfer technique that enables the transmission of electrical energy through an electromagnetic field, eliminating the need for physical connections [2–4]. This concept was initially proposed and patented by Nikola Tesla in the early 20th century [3, 5–7], sparking scientific interest and research in WPT systems over the past century.

Masers and the maser communication system marked the initial milestones in the development of far-field Wireless Power Transfer (WPT) systems in 1960 [8]. Within a decade, lasers emerged as a viable solution for far-field WPT applications [9]. Moreover, in 1969, William C. Brown invented a microwave WPT system [10]. Despite the height constraint of 15.44 m, Brown successfully transferred 270 W of power via microwave to a prototype aircraft [11]. Kimura et al. proposed a miniature opto-electric transformer for optical WPT approaches [12]. Sahai and Graham suggested a device incorporating a laser-diode array for optical WPT systems [13]. Ishiyama et al. explored the use of an ultrasonic air transducer for WPT

[14]. Approximately a century after Tesla's initial presentation, Kurs et al. introduced and conducted experiments with a novel Resonant Inductive Coupling Wireless Power Transfer (RIC-WPT) system. Led by Professor M. Soljačić, this research team achieved the transfer of 60 W of power with an efficiency of 40% over a distance exceeding 2 m between the transmitter and receiver [15]. Following this significant advancement, the interest in WPT has been further amplified.

Canon et al. used only one transmitter coil for multiple loads [16]. Karakaya transferred power to the DC motor with 60% efficiency by WPT. He also sent the motor rotation direction information of the DC motor within this power [17].

Canon et al. employed a single transmitter coil to power multiple loads in their study [16]. Karakaya successfully achieved power transfer to a DC motor with an efficiency of 60% using WPT. Additionally, he transmitted information about the rotational direction of the DC motor alongside the power transfer [17].

Over time, researchers have proposed various strategies to enhance the efficiency of WPT systems. These approaches encompass the utilization of auxiliary coils [4, 18–20], the development of novel mathematical models [21–25], the design of advanced control circuits [1, 26–29], the application of machine learning techniques [30–35], and the modification of geometric structures [36–43]. These endeavours have aimed to optimize the performance and effectiveness of WPT systems in an academic and formal context.

In the past two decades, there has been a remarkable surge in the popularity of electric vehicles, consequently creating a new realm for Wireless Power Transfer (WPT) systems. This development has attracted the attention of numerous researchers and prominent technology companies, leading to extensive exploration and advancements in this emerging field [44–49].

This paper introduces a parametric optimization and normalization methodology for coreless Resonant Inductive Coupling Wireless Power Transfer (RIC-WPT) systems. The proposed system is built upon a series-series (SS) compensated circuit utilizing flat spiral coils, operating at a frequency of 86 kHz. The selection of this specific operating frequency aligns with the standard set forth by the Society of Automotive Engineers (SAE) in their SAE J2954 guidelines.

2. Classifying of Wireless Power Transfer

In wireless power transfer (WPT) systems, the notion of a "media" or "carrier field" arises, representing the energy form through which power is converted and transmitted. Based on the investigations conducted, WPT systems can be categorized into distinct research domains, as depicted in Figure 1, depending on the type of carrier field employed [47], [50, 51].

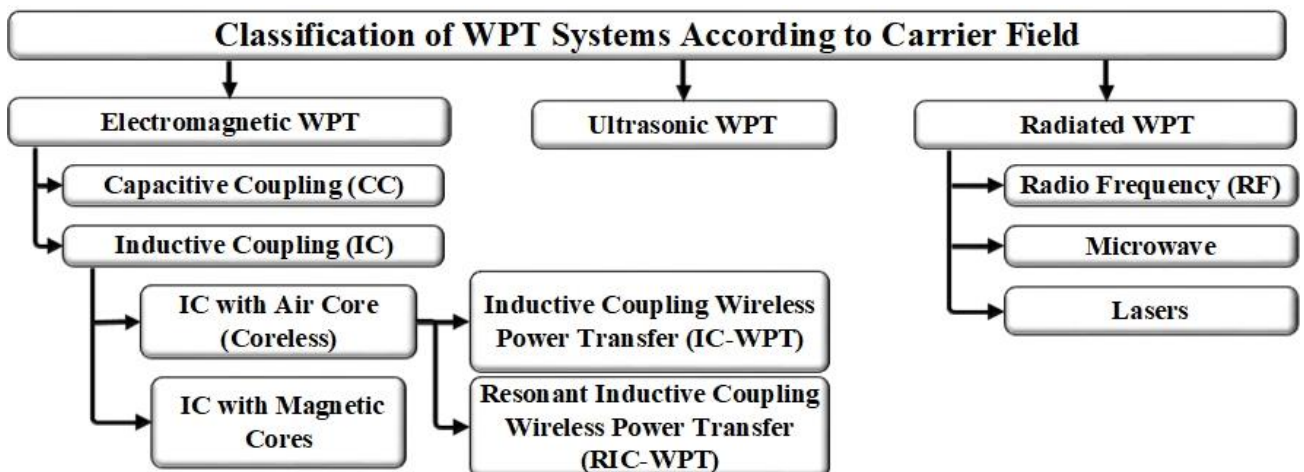


Figure 1. Classification of WPT systems according to carrier field [52].

Additionally, the power transfer distance serves as a crucial parameter for classifying Wireless Power Transfer (WPT) systems. Therefore, WPT systems can be categorized into distinct research areas, as illustrated in Figure 2 [47, 53, 54].

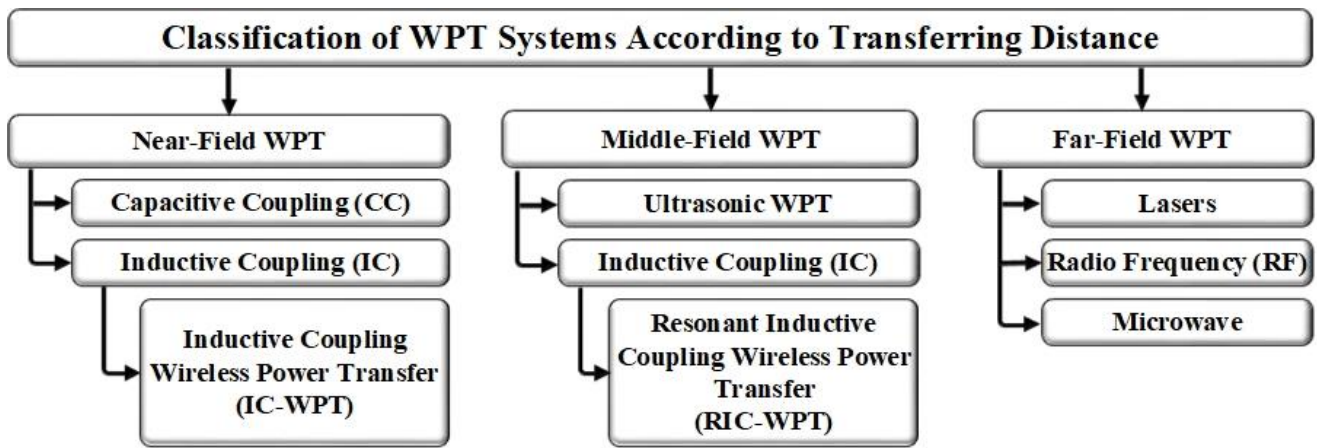


Figure 2. Classification of WPT systems according to transferring distance [52].

Simultaneously, Wireless Power Transfer (WPT) systems can be classified based on the number of loads and sources they involve. Circuits with a single source and a single load are referred to as Single Input - Single Output (SISO). Similarly, circuits with a single source and multiple loads are categorized as Single Input - Multiple Output (SIMO). On the other hand, circuits with multiple sources and a single load are termed as Multiple Input - Single Output (MISO), and circuits with multiple sources and multiple loads fall under the classification of Multiple Input - Multiple Output (MIMO) [55]. Figure 3 illustrates these circuit models, where "Tx" represents the transmitter circuit, "Rx" represents the receiver circuit, " R_s (Ω)" denotes the source resistance, " C_t (F)" signifies the resonant capacitor of the transmitter, " L_t (H)" represents the transmitter coil, " R_t (Ω)" signifies the inner resistance of the transmitter coil, " L_r (H)" represents the receiver coil, " R_r (Ω)" signifies the inner resistance of the receiver coil, " C_r (F)" denotes the resonant capacitor of the receiver circuit, " R_L (Ω)" represents the load, and "M (H)" stands for mutual inductance.

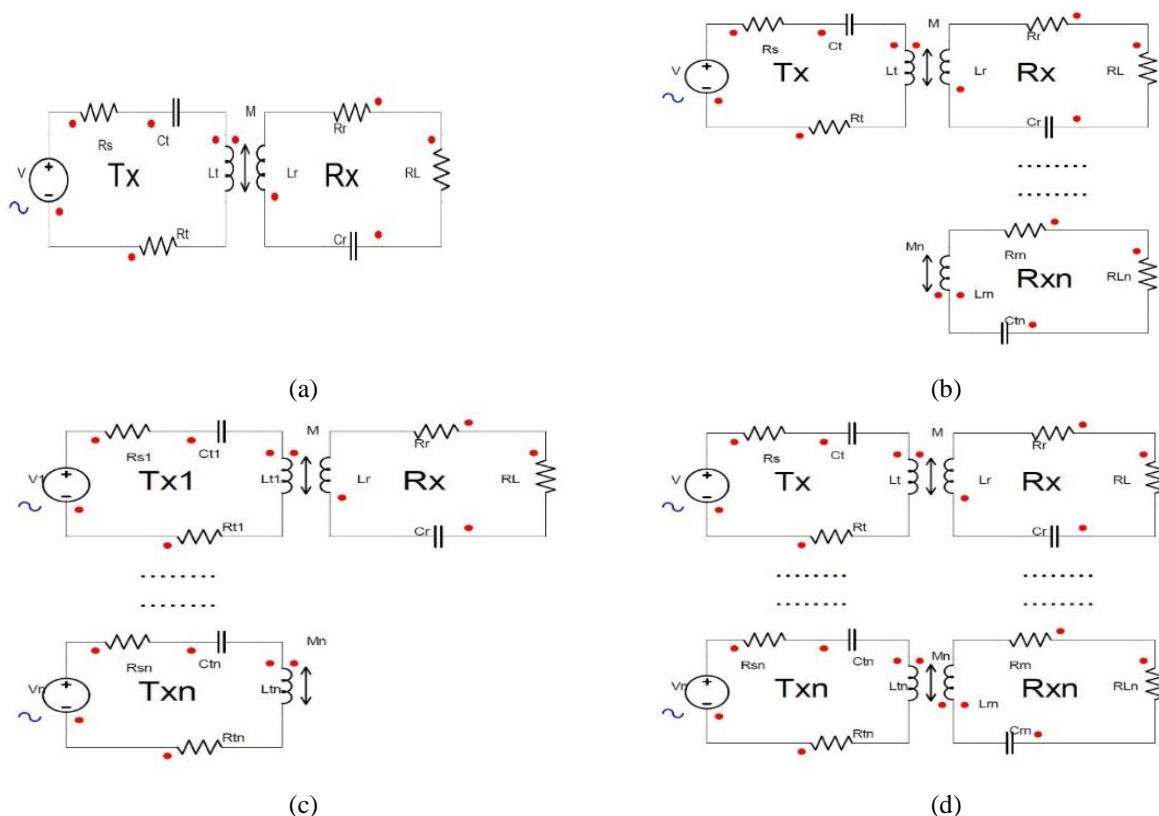


Figure 3. Circuit models of WPT systems, (a) SISO circuit model, (b) SIMO circuit model, (c) MISO circuit model, (d) MIMO circuit model.

The final parameter for categorizing WPT systems is the compensation type employed in the transmitter and receiver circuits. There exist four fundamental types of compensation: Serial Transmitter - Serial Receiver (SS), Serial Transmitter - Parallel Receiver (SP), Parallel Transmitter - Serial Receiver (PS), and Parallel Transmitter - Parallel Receiver (PP) compensated circuit models [21, 47]. Figure 4 illustrates these circuit models.

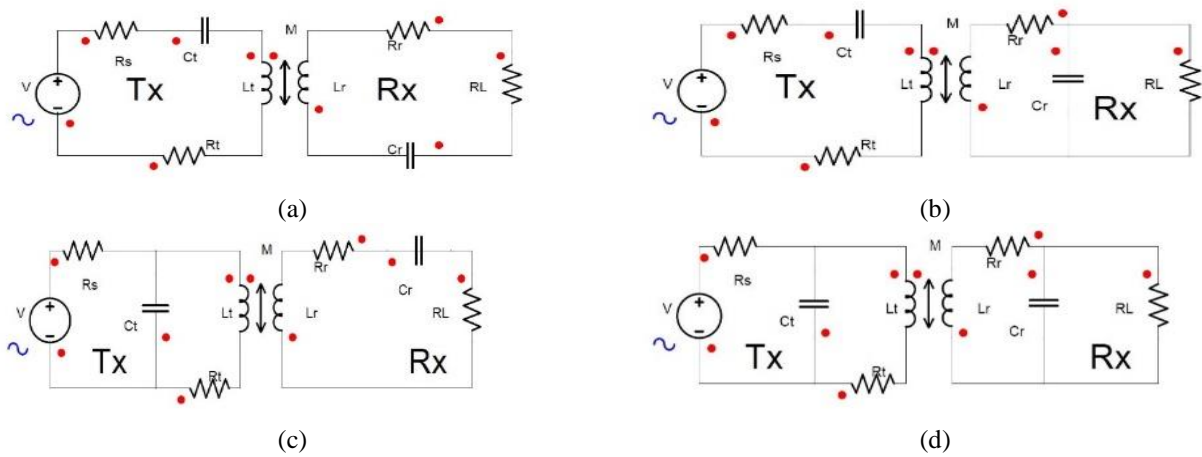


Figure 4. Circuit models of WPT systems, (a) SS compensated circuit, (b) SP compensated circuit, (c) PS compensated circuit, (d) PP compensated circuit.

3. Modelling of the WPT Circuit

The modelling of wireless power transfer involves an initial examination of the fundamental circuit equations. Subsequently, comprehensive calculations, design, and analysis of the employed WPT system have been conducted.

The Basic Equations for WPT

The concept behind the RIC-WPT system revolves around the utilization of capacitors and coils during the resonance period. During this phase, the capacitive reactance (X_C) is equated to the inductive reactance (X_L). The angular frequency (ω_0) at the point of resonance can be determined using Equation 1:

$$X_L = X_C \Rightarrow \omega_0 L = \frac{1}{\omega_0 C} \Rightarrow \omega_0 = \frac{1}{\sqrt{LC}} \tag{1}$$

The resonant frequency (f_0) is given in Eq. 2:

$$\omega_0 = 2\pi f_0 = \frac{1}{\sqrt{LC}} \Rightarrow f_0 = \frac{1}{2\pi\sqrt{LC}} \tag{2}$$

Also, Figure 5 illustrates two magnetically interconnected coils and the overall system they comprise [4], [56]. The transfer of power occurs from inductor L_1 to inductor L_2 through magnetic coupling.

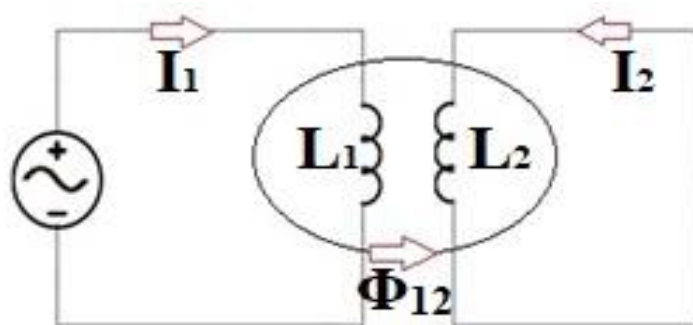


Figure 5. Two coils magnetically connected by common flux Φ_{12} [4, 56]

The magnetic flux, denoted as Φ_{12} (Wb), originates from the current I_1 (A). However, the presence of the L_2 coil has a significant impact on the overall system. As a result, the magnetic flux Φ_{12} (Wb) undergoes a constant change, as described in Eq. 3. This constant is referred to as "Mutual Inductance," with its SI unit being Henry (H), symbolized by M , as indicated in Eq.3 [57].

$$\Phi_{12} = M.I_1 \quad (3)$$

Through extensive research on Wireless Power Transfer (WPT), practical methodologies have been developed to calculate the mutual inductance based on the specific geometric configurations employed. Equation 4 represents the mathematical expression utilized for determining the mutual inductance in the context of two single-winding wire coils. In this equation, denoted as Eq.4 [46, 52, 58–62], M_0 (μH) represents the mutual inductance, while a (m) and b (m) correspond to the radii of the transmitter and receiver coils, respectively. Furthermore, $K(c)$ and $E(c)$ denote the complete elliptic integrals of the first and second order, respectively, with respect to the parameter c .

$$M_0 = \mu_0 \frac{\sqrt{ab}}{\sqrt{c}} [(2-c)K(c) - 2E(c)] \quad (4)$$

Where d (m) is the distance between transmitter and receiver coils as given in Eq.5:

$$c = \frac{4ab}{(a+b)^2 + d^2} \quad K(\varphi, c) = \int_0^\varphi \frac{d\varphi}{\sqrt{1-c^2 \cdot \sin^2 \varphi}} \quad E(\varphi, c) = \int_0^\varphi \sqrt{1-c^2 \cdot \sin^2 \varphi} \cdot d\varphi \quad (5)$$

Thus, Eq.4 provides the mutual inductance between two single-turn loops. However, for coils with multiple turns, denoted by N_1 and N_2 representing the number of turns, the mutual inductance M is given by Eq.6.

$$M = M_0 N_1 N_2 \quad (6)$$

In WPT systems, there is another constant which expresses the effectiveness of the magnetic coupling between the coils to indicate how much of the transmitted power, that is, the flux, reaches the receiver. This constant is called the coupling coefficient. This constant is denoted by the letter “ k ” [56]. k takes values between 0 and 1 and is defined as given in Eq.7: In Wireless Power Transfer (WPT) systems, the efficacy of the magnetic coupling between the coils, which determines the proportion of transmitted power (flux) received by the receiver, is quantified by a parameter known as the coupling coefficient. The coupling coefficient is denoted by the symbol “ k ” [56]. It assumes values between 0 and 1 and is mathematically defined as shown in Eq.7.

$$k = \frac{M}{\sqrt{L_t L_r}} \quad (7)$$

Calculation of the WPT Coils

Previous literature has documented various coil shapes, such as the conventional rectangular coil, rectangular double loop coil, hexagonal coil, and cloverleaf, in the context of wireless power transfer (WPT) systems. The geometric configuration of the coils employed in WPT circuits significantly impacts their performance [63]. In this study, flat spiral coils are utilized as both transmitter and receiver coils, as depicted in Figure 6.

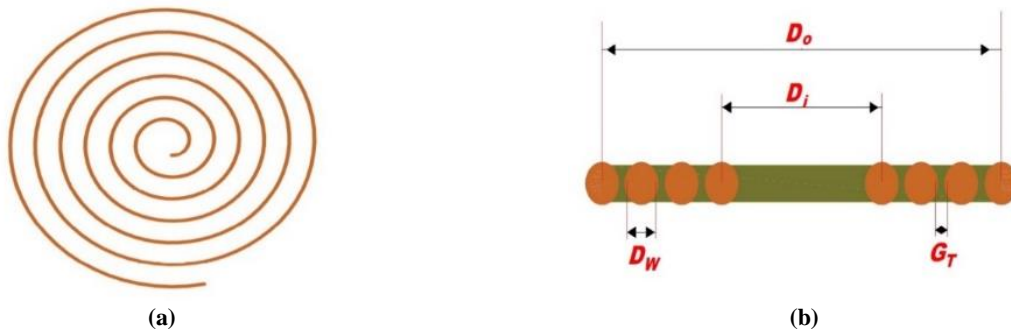


Figure 6. The geometric structure of the WPT coils, (a) Flat spiral coil, (b) Flat spiral coil variables [52].

The inductance of the coil, L (μH), is defined [4, 52, 64–66] as seen in Eq.8:

$$A = \frac{D_i + N(D_w + G_T) - G_T}{2}; L = \frac{N^2 \cdot A^2}{30 \cdot A - 11 \cdot D_i} (\mu H) \quad (8)$$

The inside diameter of the coil, denoted as D_i (m), along with the wire diameter represented by D_w (m), and the distance between wire turns, indicated as G_T (m), are crucial parameters. Additionally, the number of turns is denoted by N . The length of the wire used in the coil, l_w (m), can be calculated using Eq. 9 [66].

$$l_w = \beta \frac{\pi}{2} N(D_i + D_o) \quad (9)$$

β is the twist factor coefficient which is 1.02 [65]. D_o (m) is the outer diameter of the coil and defined [66] by Eq.10:

$$D_o = [D_i + 2N(D_w + G_T) - 2G_T] \quad (10)$$

The DC resistance, R_{DC} (Ω), of a wire, where (S/m) is the electrical conductivity, and A_w (m^2) is the area of the wire cross-sectional area, is calculated [57, 67] by Eq.11:

$$R_{DC} = \frac{l_w}{\sigma \cdot A_w} \quad (11)$$

The frequency could be easily added to calculations with the use of electrical conductivity. Because the skin depth, δ (m), and the electrical conductivity, (S/m) , are related to each other [57] by Eq.12:

$$\delta = \frac{1}{\sqrt{\pi f \mu \sigma}} \quad (12)$$

Where μ (H/m), is the magnetic permeability, and f (Hz) is the frequency. Thus the total resistance of the coil, R_w (Ω), is calculated by Eq.13:

$$R_w = \frac{l_w}{\sigma A_w} \left(\frac{1}{4} + \frac{r_w}{2\delta} \right) \quad (13)$$

Design of the Circuit

In this research, the resonant inductive coupling wireless power transmission (RIC-WPT) method is employed, utilizing the series-series (SS) compensated and single-input single-output (SISO) circuit model depicted in Figure 4(a). The circuit analysis is conducted using the equivalent circuit model illustrated in Figure 7. The variable I_s (A) represents the current in the transmitter circuit, while I_L (A) denotes the current in the receiver circuit.

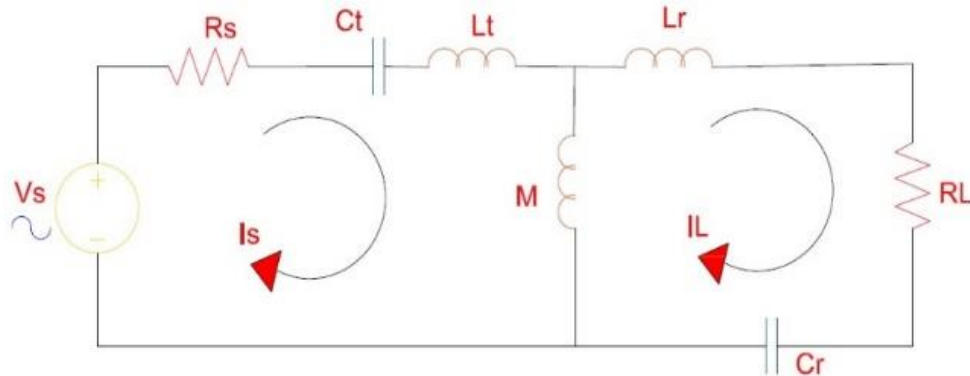


Figure 7. Equivalent circuit model of the WPT system [21–23, 41].

According to Kirchhoff's voltage law, we can express, as stated in Eq.14 [52] for Figure 7:

$$\begin{pmatrix} V_S \\ 0 \end{pmatrix} = \begin{pmatrix} R_S + j\left(\omega L_t - \frac{1}{\omega C_t}\right) & -j\omega M \\ -j\omega M & R_L + j\left(\omega L_r - \frac{1}{\omega C_r}\right) \end{pmatrix} \cdot \begin{pmatrix} I_S \\ I_L \end{pmatrix} \quad (14)$$

At the resonant moment ($X_C = X_L$) with Eqs.15-16, and the efficiency (η) of the WPT system in Eq.17:

$$I_S = \frac{V_S \cdot (R_L + R_r)}{R_t \cdot (R_L + R_r) + \omega^2 M^2} \quad (15)$$

$$I_L = -\frac{j\omega M V_S}{R_t \cdot (R_L + R_r) + \omega^2 M^2} \quad (16)$$

$$\eta = \left(\frac{I_L}{I_S}\right)^2 \cdot \frac{(R_L + R_r)}{Z_t} = \frac{\omega^2 M^2}{R_t \cdot (R_L + R_r) + \omega^2 M^2} \quad (17)$$

4. Simulation Studies

Before conducting the simulation studies, initial values were determined and listed in Table 1. Subsequently, a Matlab code is developed with parametric values based on the number of turns of the coils, aiming to design the most efficient coil system.

Table 1. Known initial values of the design.

Description	Symbol	Value
The operating frequency	f	86 kHz
The diameter of the wire	D_w	16 mm
The voltage of the source	V_s	12 V
Load	R_L	5 Ω
The distance between the coil turns	G_t	3 mm
The inside diameter of the coil	D_i	10 mm

The number of turns of the transmitter coil is denoted as N_t , while the number of turns of the receiver coil is denoted as N_r , as indicated in Table 2.

Table 2. Parametric values of the WPT coils.

Parameters	N_t	N_r
Parametric Range	5-10	5-20
Linear Step	5	5

After the calculations, it is determined that the most efficient winding number was obtained when $N_r = 20$ and $N_t = 10$. I_s (A) is the transmitter circuit current, I_L (A) is the receiver circuit current, V_L (V) is the voltage value on the load, P_i (W) is the input power, P_o (W) is the output power, and η (%) is the efficiency in Table 3.

Table 3. The most efficient number of the turns of the coils.

N_t	N_r	L_t (uH)	L_r (uH)	I_s (A)	I_L (A)	V_L (V)	P_i (W)	P_o (W)	η (%)
10	20	13.4263	103.5367	70.6	12.59	62.96	847	793	93.61

The coil system design is created in 3D using the calculated values within the model specified in the ANSYS-Electronics-Maxwell software. Figure 8 illustrates the complete coil system, with the receiver coil represented by the larger coil and the transmitter coil represented by the smaller coil.

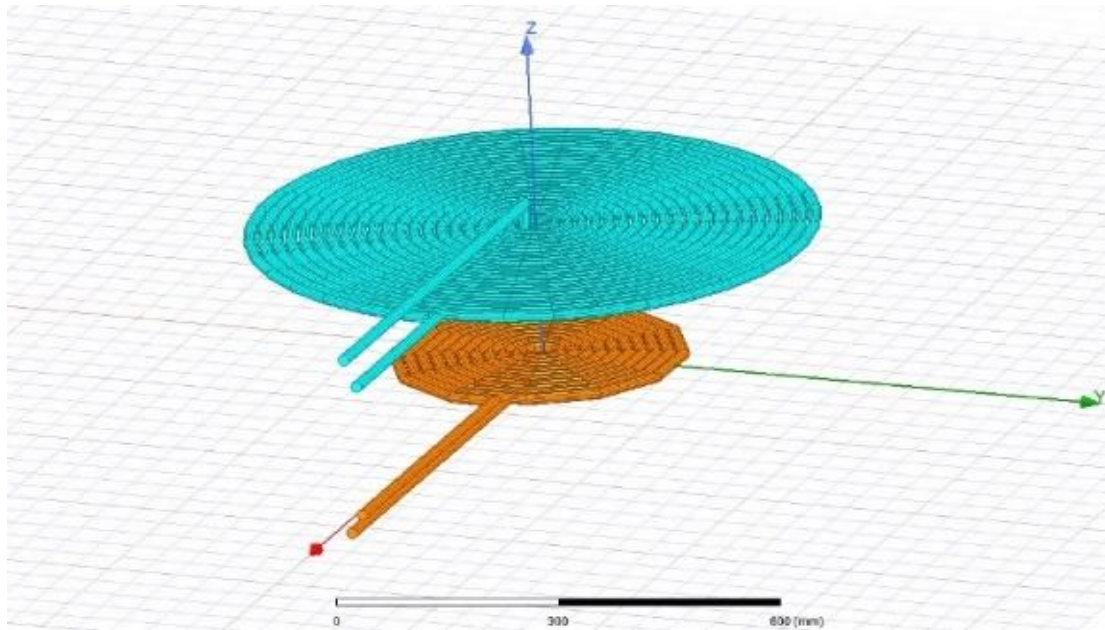


Figure 8. Maxwell 3D coil system

The spacing between the coils, denoted as 'z_space' (mm), is systematically varied from 50 mm to 500 mm with a linear increment of 50 mm. In wireless power transfer (WPT) systems, there exists a linear relationship between efficiency and the coupling coefficient. Hence, the impact of the spacing, as depicted in Figures 9 and 10, on the coupling coefficient and mutual inductance is investigated.

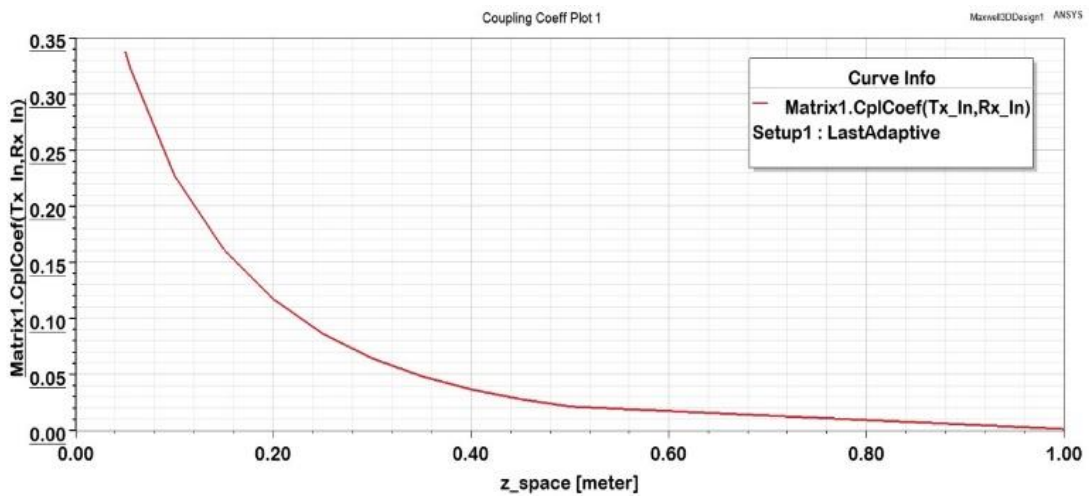


Figure 9. The parametric effect of the distance on the coupling coefficient.

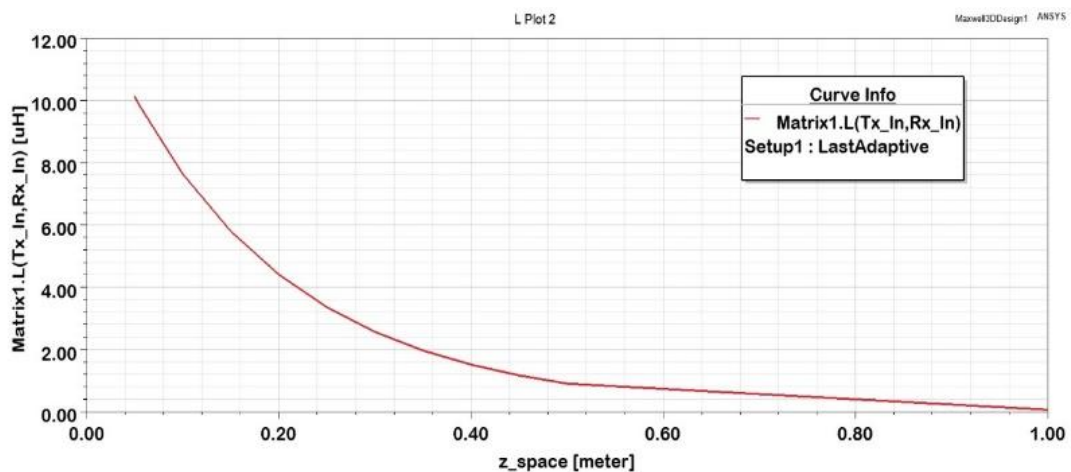


Figure 10. The parametric effect of the distance on the mutual inductance.

Table 4 illustrates the variation of values about distance, showcasing the dynamic nature of the designed coil system. Subsequently, the coil system is integrated into the power electronics circuit, which is developed using ANSYS-Simplorer software, allowing for co-simulation with ANSYS-Maxwell. The comprehensive WPT system is depicted in Figure 11.

Table 4. Effect of the distance on mutual inductance and coupling coefficient

z_space (mm)	50	100	150	200	250	300	350	400	450	500	1000
M(uH)	10.12	7.64	5.80	4.41	3.36	2.57	1.97	1.52	1.18	0.917	0.081
k	0.337	0.227	0.161	0.117	0.086	0.064	0.048	0.037	0.028	0.021	0.0018

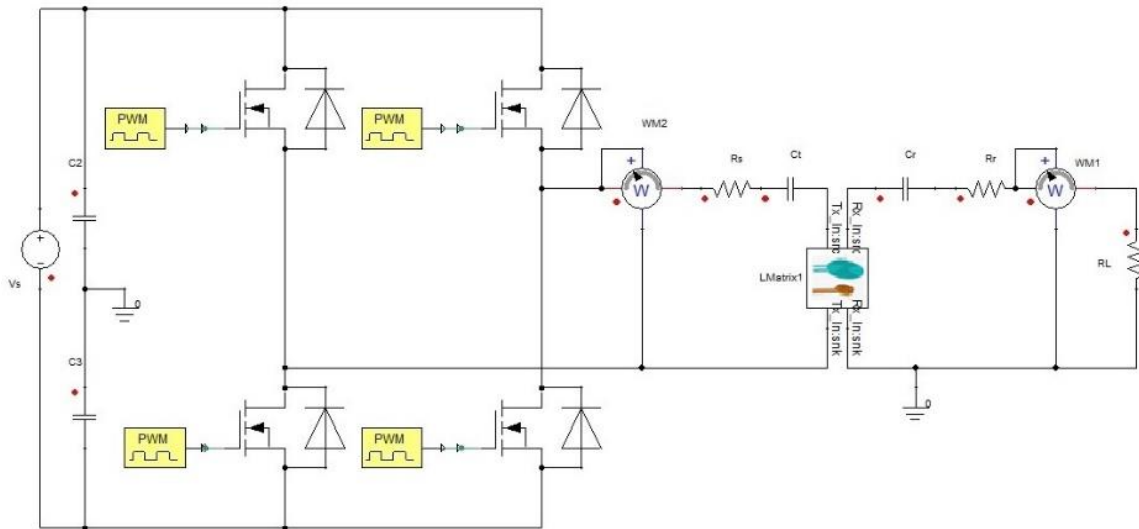


Figure 11. Power electronics circuit of the entire WPT system [41].

Initially, the circuit is co-simulated using calculated values in MATLAB. Both the input power and output power are observed during the simulation. Figure 12 depicts the input power [Pi (W)], while Figure 13 illustrates the output power [Po (W)].

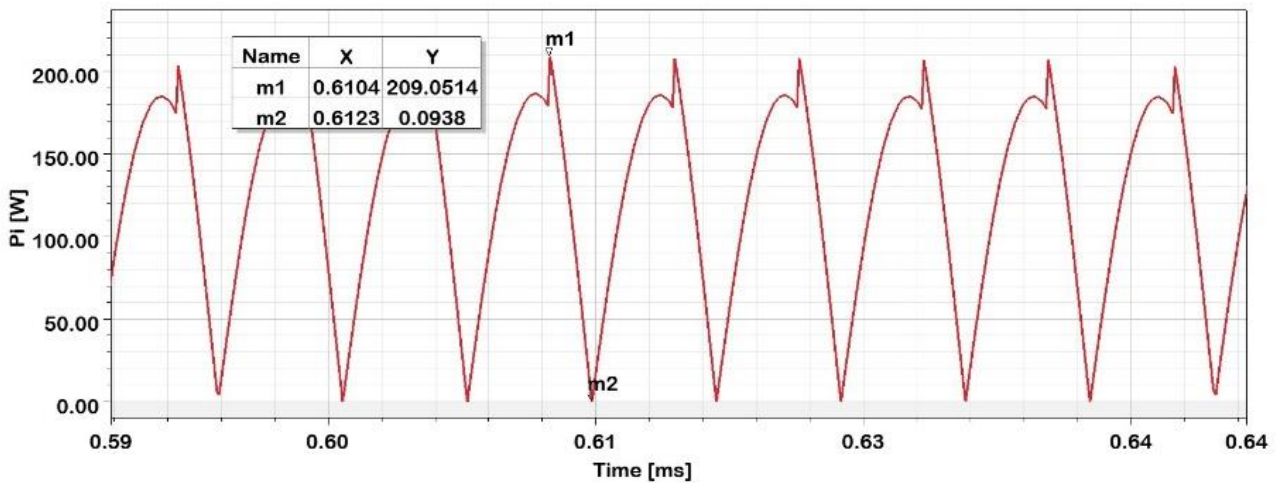


Figure 12. Pi (W) with calculated values co-simulation result.

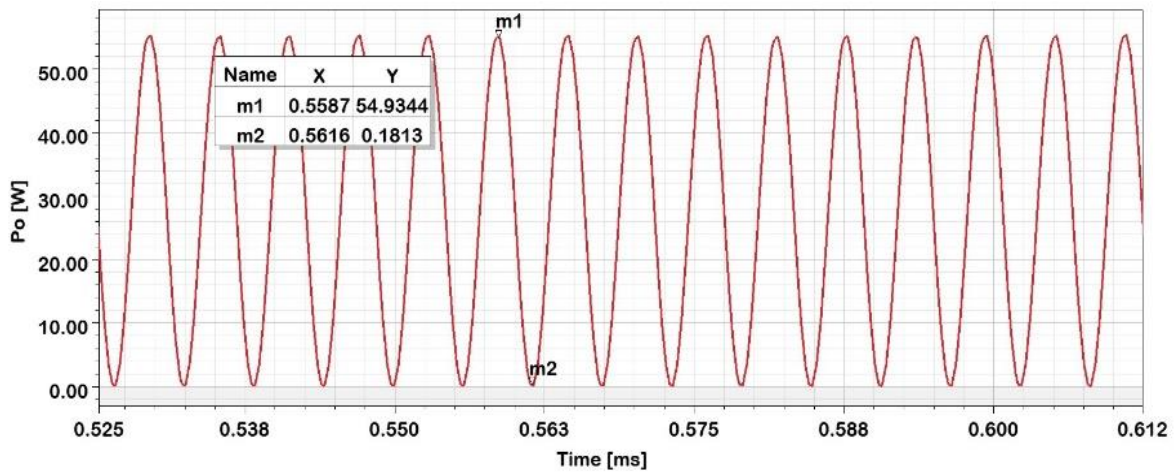


Figure 13. P_o (W) with calculated values co-simulation result.

Table 5 displays the observed values and corresponding efficiency in this case. Additionally, for the parametric studies, four variables have been chosen: capacitors (C_t , C_r), the distance between coils (z_space), operating frequency (f), and load (R_L). All these variables, along with their respective parameter values, are presented in Table 6.

Table 5. The results observed in the study which is made with the calculated values.

Variables	Values	Units
C_t	255.086	nF
C_r	33.078	nF
P_i	200	W_p
P_o	55	W_p
η (%)	27.5	

Table 6. WPT parametric values.

Variable Names	Calculated Values	Units	Parametric Range	Linear Step
z_space	200	mm	50 - 500	50
f	86	kHz	70 - 100	1
R_L	5	Ω	1 -20	1
C_t	255	nF	175 - 325	5
C_r	33	nF	20 - 150	5

Therefore, a total of 5,189,400 distinct possibilities are intended to be explored in this study. However, due to the limitation of ANSYS-Simplorer software, which can handle a maximum of 32,000 possibilities, the study has to be divided into four parts. The initial part focuses on the normalization of capacitor values. Figure 14 illustrates the relationship between efficiency and variations in capacitor values.

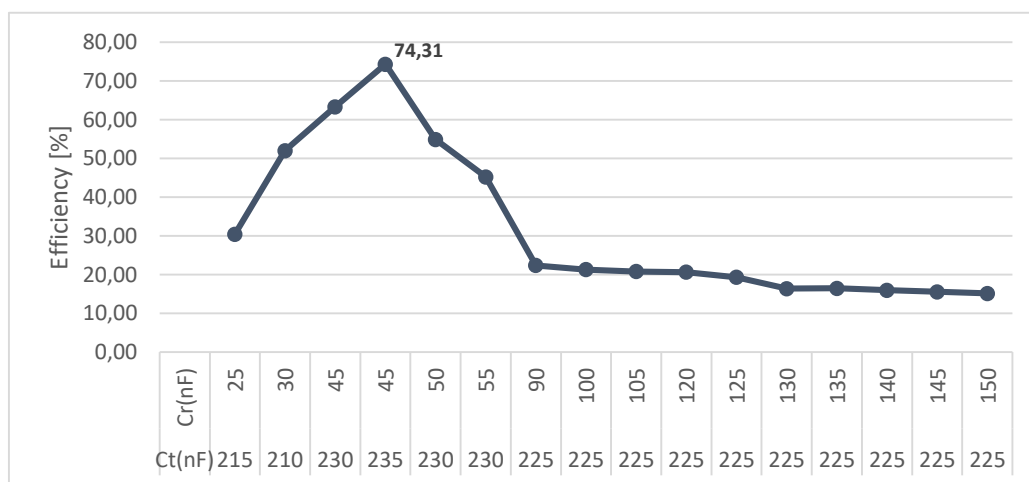


Figure 14. Efficiency characteristic vs. the parametric capacitor values.

The subsequent stage involves determining the optimal distance between coils (z_{space}) for achieving maximum efficiency. The capacitor values obtained from the previous phase are utilized in this analysis. The relationship between efficiency and distance variation is illustrated in Figure 15.

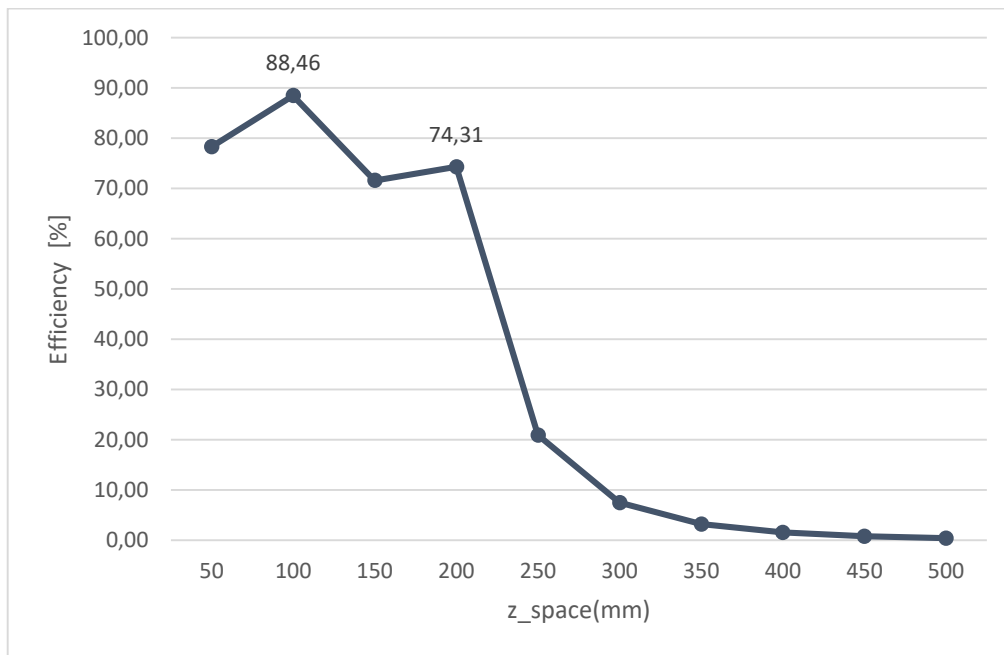


Figure 15. Efficiency characteristic vs. the parametric z_{space} (mm) values.

The optimal distance, as indicated in Table 7, for achieving the highest efficiency is 100 mm. Nevertheless, it should be noted that the output power reaches its maximum value when the distance between the coils is set to 200 mm.

Table 7. Efficient and power values for different z_{space} values

z_{space} (mm)	P_1 (W _{rms})	P_0 (W _{rms})	η (%)
100	72.56	64.19	88.46
200	519.29	385.89	74.31

The third phase of the study involves altering the load value while keeping the chosen capacitor values and the optimal z_{space} value constant. This enables the easy observation of the efficiency variation in response to changes in the load. Figure 16 illustrates the relationship between efficiency and load variations, allowing for straightforward analysis.

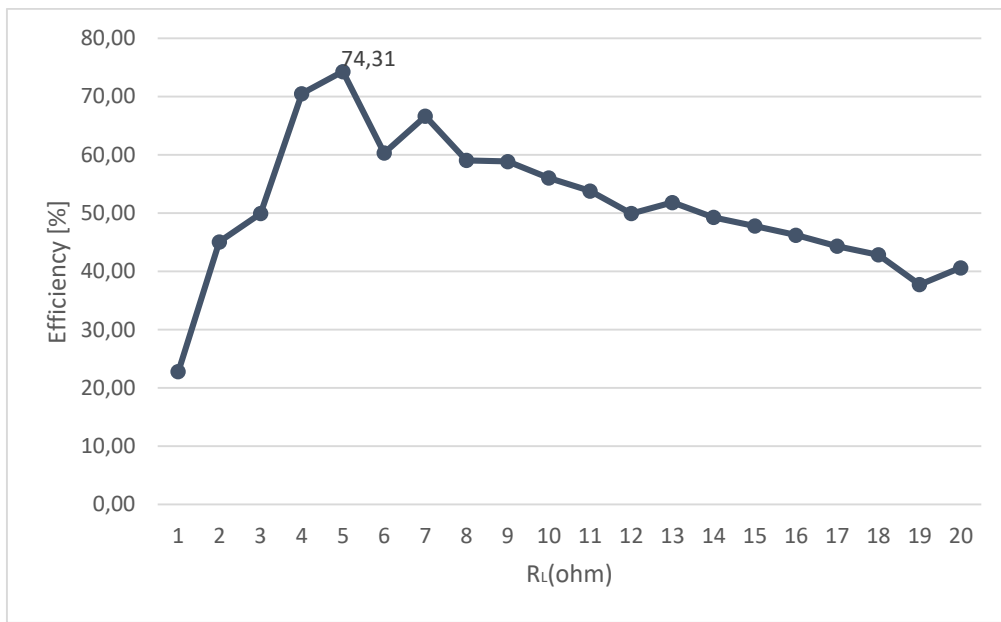


Figure 16. Efficiency characteristic vs. the parametric z_space (mm) values.

The fourth phase of the study involves the determination of the operating frequency, with all other parameters having been established. The operating frequency has been analyzed based on both calculated values and empirical observations. Figure 17 illustrates the relationship between the output power and various frequency values using the calculated capacitor values.

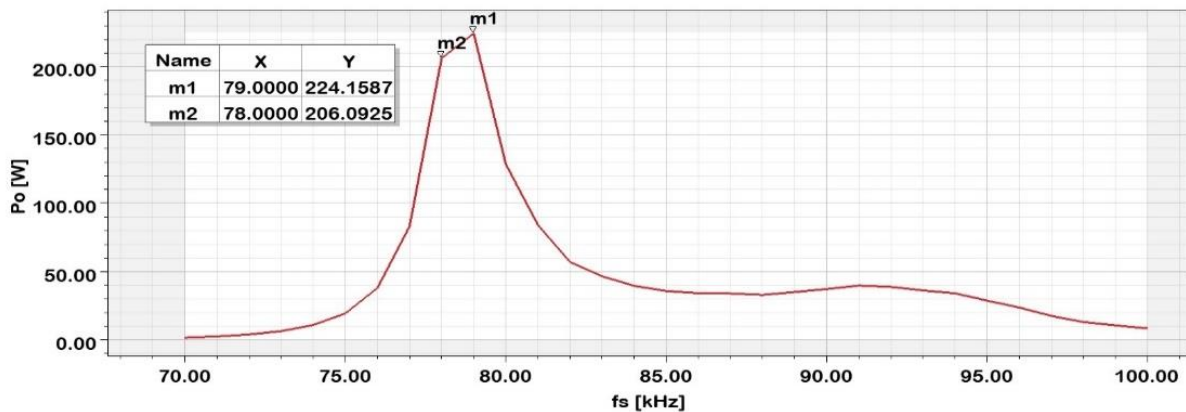


Figure 17. Po (W) vs. the parametric frequency values with calculated capacitor values.

Likewise, Figure 18 shows the output power with the determined capacitor values against different frequency values.

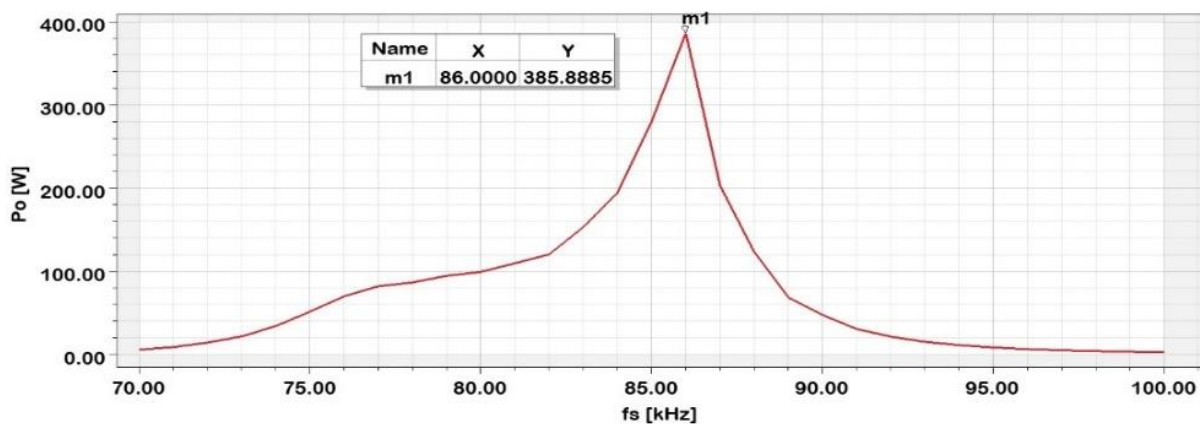


Figure 18. Po (W) vs. the parametric frequency values with calculated capacitor values.

Lastly, a final simulation was conducted to assess the benefits of the parametric approach. A new power electronics circuit was designed in ANSYS-Simplorer, omitting the co-simulation aspect. Subsequently, the circuit was simulated using Simplorer' built-in components. The efficiency results of the three studies are presented in Table 8.

Table 8. The comparison of the results.

Studies	P_i (W _{rms})	P_o (W _{rms})	η (%)
Calculation result	847	793	93.61
Results without co-simulation	848.52	594	70.39
Results with Parametrically co-simulation	519.29	385.88	74.31

The efficiency for WPT is highly affected by parameters such as the distance between transmit and receive coils, the coupling coefficient and resonance. Compared with the estimation studies based on simulations with parameters such as distance between the coils, alignment errors, in the studies conducted for the estimation of the efficiency [32, 41, 47]. Also, the efficiency value obtained in this study, with a rate of approximately 75%, suggests the parametric simulation approach as a very useful method for designers. Essentially, the efficiency does not depend only on the design of the coils and the distances between them. The efficiency of the power electronics circuit is very effective in this regard and should be considered together with the coil design.

5. Conclusion

This study introduces and analyses a wireless power transfer model through the process of definition, design, and parametric analysis. The system design calculations are performed using Matlab software in a parametric manner. It is observed that the results obtained from the equations used for calculations related to the flat spiral coil, mutual inductance, and coupling coefficient align closely with the simulation results. As a result, it is concluded that these equations can be effectively employed in future research on wireless power transfer.

The proposed method for WPT design demonstrates superior efficiency compared to the components available in ANSYS-Simplorer software and offers the advantage of simplified implementation with standardized components. Moreover, contrary to the conventional assumption that increasing the current on the transmitter side would lead to increased power on the receiver side, different outcomes have been obtained. It is determined that the power electronics circuit elements, correctly identified through parametric analysis, draw less current from the power source.

As a foundation for future studies in the field, it has been established that the design and operation of the coil should be conducted through co-simulation, while the determination of power electronics components should be based on parametric analysis using the computed outcomes. It is worth noting that, to achieve a constant load, all circuit parameters should be adjusted or normalized concerning a specific value.

Competing Interest / Conflict of Interest

The authors declare that they have no competing interests.

Author Contribution

We declare that all Authors equally contribute.

6. References

- [1] Konishi, A., Umetani, K., & Hiraki, E. (2018, May). High-frequency self-driven synchronous rectifier controller for WPT systems. In 2018 International Power Electronics Conference (IPEC-Niigata 2018-ECCE Asia) (pp. 1602-1609). IEEE.
- [2] Siddiqui, A., Nagani, A., & Ali, R. (2015). Wireless power transfer techniques: a review. *Recent & Innovation Trends in Computing & Communication*, 3(12), 6711-616.
- [3] Tesla, N. (1905). *Art of Transmitting Electrical Energy through the Natural Medium*.
- [4] Nisshagen, M., & Sjöstrand, E. (2017). Wireless power transfer using resonant inductive coupling-Design and implementation of an IPT system with one meter air gap in the region between near-range and mid-range..
- [5] Tesla, N. (1900). *System of Transmission of Electrical Energy*, pp. 1–6, [Online]. Available: <https://patentimages.storage.googleapis.com/62/90/92/45a5932052a940/US645576.pdf>
- [6] Tesla, N. (1900). *Apparatus for Transmission of Electrical Energy*.
- [7] Tesla, N. (1898). "High Frequency Oscillators for Electro-Therapeutic and Other Purposes," *Proc. IEEE*, 87(7), 1282.
- [8] Schawlow, A. L., & Townes, C. H. (1960). U.S. Patent No. 2,929,922. Washington, DC: U.S. Patent & Trademark Office.

- [9] Maiman, T. H. (1967). Ruby laser system, pp. 3, 353, 115.
- [10] Brown, W.C., (1969). Microwave to DC Converter.
- [11] Brown, W.C. (1965). Experimental Airborne Microwave Supported Platform.
- [12] Kimura, M., Miyakoshi, N., & Daibou, M. (1991, January). A miniature opto-electric transformer. In [1991] Proceedings. IEEE Micro Electro Mechanical Systems (pp. 227-232). IEEE.
- [13] Sahai, A., & Graham, D. (2011, May). Optical wireless power transmission at long wavelengths. In 2011 International Conference on Space Optical Systems & Applications (ICSOS) (pp. 164-170). IEEE.
- [14] Ishiyama, T., Kanai, Y., Ohwaki, J., & Mino, M. (2003, October). Impact of a wireless power transmission system using an ultrasonic air transducer for low-power mobile applications. In IEEE Symposium on Ultrasonics, 2003 (Vol. 2, pp. 1368-1371). IEEE.
- [15] Kurs, A., Karalis, A., Moffatt, R., Joannopoulos, J. D., Fisher, P., & Soljacic, M. (2007). Wireless power transfer via strongly coupled magnetic resonances. *science*, 317(5834), 83-86.
- [16] Cannon, B. L., Hoburg, J. F., Stancil, D. D., & Goldstein, S. C. (2009). Magnetic resonant coupling as a potential means for wireless power transfer to multiple small receivers. *IEEE transactions on power electronics*, 24(7), 1819-1825.
- [17] Karakaya, U. (2007). Motor Control Via Wireless Energy & Information Transfer, M.Sc. Thesis, Institute of Science & Technology, Istanbul Technical University, Türkiye.
- [18] Sample, A. P., Meyer, D. T., & Smith, J. R. (2010). Analysis, experimental results, & range adaptation of magnetically coupled resonators for wireless power transfer. *IEEE Transactions on industrial electronics*, 58(2), 544-554.
- [19] Koma, R., Nakamura, S., Ajisaka, S., & Hashimoto, H. (2011, July). Basic analysis of the circuit model using relay antenna in magnetic resonance coupling position sensing system. In 2011 IEEE/ASME International Conference on Advanced Intelligent Mechatronics (AIM) (pp. 25-30). IEEE.
- [20] Cheon, S., Kim, Y. H., Kang, S. Y., Lee, M. L., Lee, J. M., & Zyung, T. (2010). Circuit-model-based analysis of a wireless energy-transfer system via coupled magnetic resonances. *IEEE Transactions on Industrial Electronics*, 58(7), 2906-2914.
- [21] Wang, C. S., Covic, G. A., & Stielau, O. H. (2004). Power transfer capability & bifurcation phenomena of loosely coupled inductive power transfer systems. *IEEE transactions on industrial electronics*, 51(1), 148-157.
- [22] Sallán, J., Villa, J. L., Llombart, A., & Sanz, J. F. (2009). Optimal design of ICPT systems applied to electric vehicle battery charge. *IEEE Transactions on Industrial Electronics*, 56(6), 2140-2149.
- [23] Chopra, S., & Bauer, P. (2011, October). Analysis & design considerations for a contactless power transfer system. In 2011 IEEE 33rd International Telecommunications Energy Conference (INTELEC) (pp. 1-6). IEEE.
- [24] Imura, T., & Hori, Y. (2011). Maximizing air gap & efficiency of magnetic resonant coupling for wireless power transfer using equivalent circuit & Neumann formula. *IEEE Transactions on industrial electronics*, 58(10), 4746-4752.
- [25] Jang, Y. J., Suh, E. S., & Kim, J. W. (2015). System architecture & mathematical models of electric transit bus system utilizing wireless power transfer technology. *IEEE Systems Journal*, 10(2), 495-506.
- [26] Low, Z. N., Casanova, J. J., Maier, P. H., Taylor, J. A., Chinga, R. A., & Lin, J. (2009). Method of load/fault detection for loosely coupled planar wireless power transfer system with power delivery tracking. *IEEE Transactions on Industrial Electronics*, 57(4), 1478-1486.
- [27] Jadidian, J., and Katabi, D. (2014). Magnetic MIMO, (495-506).
- [28] Agcal, A., Ozcira, S., and Bekiroglu, N. (2016). Wireless power transfer by using magnetically coupled resonators. *Journal of Wireless Power Transfer: Fundamentals and Technologies*, 49-66.
- [29] Ozdemir, C. (2017). Adaptive Control System Design and Implementation for Power Quality and Power Transfer Efficiency at Wireless Power Transfer Systems, M.Sc. Thesis, Institute of Science and Technology, Mersin University, Türkiye.
- [30] Jeong, S., Lin, T. H., & Tentzeris, M. M. (2019). A real-time range-adaptive impedance matching utilizing a machine learning strategy based on neural networks for wireless power transfer systems. *IEEE Transactions on Microwave Theory & Techniques*, 67(12), 5340-5347.
- [31] Bai, T., Mei, B., Zhao, L., & Wang, X. (2019). Machine learning-assisted wireless power transfer based on magnetic resonance. *IEEE Access*, 7, 109454-109459.
- [32] Ustun, D., Balci, S., & Sabanci, K. (2020). A parametric simulation of the wireless power transfer with inductive coupling for electric vehicles, & modelling with artificial bee colony algorithm. *Measurement*, 150, 107082.
- [33] Faraci, G., Raciti, A., Rizzo, S. A., & Schembra, G. (2020). Green wireless power transfer system for a drone fleet managed by reinforcement learning in smart industry. *Applied Energy*, 259, 114204.
- [34] Kim, J., Clerckx, B., & Mitcheson, P. D. (2020). Signal & system design for wireless power transfer: Prototype, experiment & validation. *IEEE Transactions on Wireless Communications*, 19(11), 7453-7469.

- [35] Gheisarnejad, M., Farsizadeh, H., Tavana, M. R., & Khooban, M. H. (2020). A novel deep learning controller for DC–DC buck–boost converters in wireless power transfer feeding CPLs. *IEEE Transactions on Industrial Electronics*, 68(7), 6379-6384.
- [36] Nam, I., Dougal, R., & Santi, E. (2012, September). Novel control approach to achieving efficient wireless battery charging for portable electronic devices. In *2012 IEEE Energy Conversion Congress & Exposition (ECCE)* (pp. 2482-2491). IEEE.
- [37] Phokhaphan, N., Choeisai, K., Noguchi, K., Araki, T., Kusaka, K., Orikawa, K., & Itoh, J. I. (2013, November). Wireless power transfer based on MHz inverter through PCB antenna. In *2013 1st International Future Energy Electronics Conference (IFEEEC)* (pp. 126-130). IEEE.
- [38] Gao, L., Hu, W., Xie, X., Deng, Q., Wu, Z., Zhou, H., & Jiang, Y. (2013, June). Optimum design of coil for wireless energy transmission system based on resonant coupling. In *2013 10th IEEE International Conference on Control & Automation (ICCA)* (pp. 190-195). IEEE.
- [39] Ahn, D., & Hong, S. (2013). A transmitter or a receiver consisting of two strongly coupled resonators for enhanced resonant coupling in wireless power transfer. *IEEE transactions on industrial electronics*, 61(3), 1193-1203.
- [40] Villar, I., Iruretagoyena, U., Rujas, A., Garcia-Bediaga, A., and de Arenaza, I. P. (2015, September). Design and implementation of a SiC based contactless battery charger for electric vehicles. In *2015 IEEE Energy Conversion Congress & Exposition (ECCE)* (pp. 1294-1300). IEEE.
- [41] Kuzey, S., Balci, S., & Altin, N. (2017). Design & analysis of a wireless power transfer system with alignment errors for electrical vehicle applications. *International journal of hydrogen energy*, 42(28), 17928-17939.
- [42] Aydin, E., Kosesoy, Y., Yildiriz, E., & Aydemir, M. T. (2018, November). Comparison of hexagonal & square coils for use in wireless charging of electric vehicle battery. In *2018 International Symposium on Electronics & Telecommunications (ISETC)* (pp. 1-4). IEEE.
- [43] Doğan, Z., Özsoy, M., & İskender, İ. (2019). Manyetik Rezonansa Dayalı Kablosuz Enerji Transferi İçin Yeni Bir Nüve Geometrisi. *Gazi University Journal of Science Part C: Design & Technology*, 7(4), 1012-1024.
- [44] Neves, A., Sousa, D. M., Roque, A., & Terras, J. M. (2011, August). Analysis of an inductive charging system for a commercial electric vehicle. In *Proceedings of the 2011 14th European Conference on Power Electronics & Applications* (pp. 1-10). IEEE.
- [45] Kusaka, K., & Itoh, J. I. (2012, October). Input impedance matched AC-DC converter in wireless power transfer for EV charger. In *2012 15th International Conference on Electrical Machines & Systems (ICEMS)* (pp. 1-6). IEEE.
- [46] Fincan, B. (2015). *Designing A Wireless Charger For Electrical Vehicles*, M.Sc. Thesis, Institute of Science & Technology, Istanbul Technical University, Türkiye.
- [47] Kuzey, S. (2017). *Design of Inductive Magnetic Coupled Power Transmission System for Electric Vehicle*, M.Sc. Thesis, Institute of Science & Technology, Gazi University, Türkiye.
- [48] Yakala, R. K., Pramanick, S., Nayak, D. P., & Kumar, M. (2021). Optimization of circular coil design for wireless power transfer system in electric vehicle battery charging applications. *Transactions of the Indian National Academy of Engineering*, 6, 765-774.
- [49] Çiçek, M., Gençtürk, M., Balci, S., & Sabanci, K. (2021). The modelling, simulation, & implementation of wireless power transfer for an electric vehicle charging station. *Turkish Journal of Engineering*, 6(3), 223-229.
- [50] Moradewicz, A. J., & Kazmierkowski, M. P. (2009). High efficiency contactless energy transfer system with power electronic resonant converter. *Bulletin of the Polish Academy of Sciences: Technical Sciences*, 375-381.
- [51] Rao¹, T. C., & Geetha, K. (2016). Categories, standards & recent trends in wireless power transfer: A survey. *Indian journal of science and technology*, 9, 20.
- [52] Cicek, M. (2022). *Modeling, Simulation and Analysis of Wireless Power Transfer*, M.Sc. Thesis, Institute of Science and Technology Karamanoglu Mehmetbey University, Türkiye.
- [53] Zheng, C. (2015). *Loosely Coupled Transformer and Tuning Network Design for High-Efficiency Inductive Power Transfer Systems*, Ph.D. Thesis, Virginia Polytechnic Institute and State University. Blacksburg, Virginia.
- [54] Khayrudinov, V. (2015). *Wireless Power Transfer system: Development and Implementation*, B.Sc. Thesis, ResearchGate, Helsinki Metropolia University of Applied Sciences.
- [55] Lu, X., Wang, P., Niyato, D., Kim, D. I., and Han, Z. (2015). Wireless charging technologies: Fundamentals, standards, and network applications. *IEEE communications surveys and tutorials*, 18(2), 1413-1452.
- [56] Coca, E. (2016). *Wireless Power Transfer - Fundamentals and Technologies*.
- [57] Cheng, D. K. (1983). *Field and Wave Electromagnetics*.
- [58] Rosa, E. B., & Grover, F. W. (1912). Formulas and tables for the calculation of mutual and self-inductance (Revised). *Bulletin of the Bureau of Standards*, 8(1), 1.
- [59] Uzun, G. (2012). *Wireless Energy Transfer*, M.Sc. Thesis, Institute of Science and Technology Ondokuz Mayıs University, Türkiye.

- [60] Mendes Duarte, R., & Klaric Felic, G. (2014). Analysis of the coupling coefficient in inductive energy transfer systems. *Active & Passive Electronic Components*.
- [61] Liu, X., Xia, C., & Yuan, X. (2018). Study of the circular flat spiral coil structure effect on wireless power transfer system performance. *Energies*, 11(11), 2875.
- [62] Oraz, A. A., & Alkaya, A. (2018). Contactless Power Transfer Methods for Electric Vehicles Charging, Ciset 2018 Cilicia International Symposium on Engineering & Technology, Mersin, Turkiye.
- [63] Zhang, Y., Yan, Z., Zhu, J., Li, S., & Mi, C. (2019). A review of foreign object detection (FOD) for inductive power transfer systems, *eTransportation*, Volume 1, 100002, <https://doi.org/10.1016/j.etrans.2019.04.002>.
- [64] Wheeler, H. A. (1928). Simple inductance formulas for radio coils. *Proceedings of the institute of Radio Engineers*, 16(10), 1398-1400.
- [65] Agcal, A. (2017). Design & Implementation of a High Efficiency Wireless Power Transfer System with A New Closed Loop Algorithm, Ph.D. Thesis, Institute of Science & Technology Yıldız Technical University, Turkiye.
- [66] Namadmalan, A., Jaafari, B., Iqbal, A., & Al-Hitmi, M. (2020). Design optimization of inductive power transfer systems considering bifurcation & equivalent AC resistance for spiral coils. *IEEE Access*, 8, 141584-141593.
- [67] Fawwaz U. R., & Ulaby, T. (2015). *Fundamentals of applied electrostatics*.